Density and temperature effects on electron mobility in gaseous, critical, and liquid ethane

Norman Gee and Gordon R. Freeman
Chemistry Department, University of Alberta, Edmonton T6G 2G2, Canada
(Received 14 January 1980)

At applied electric-field strengths below a threshold value $(E/n)_{thr}$ the mobility of electrons is independent of field strength. At strengths just above the threshold the sign of the mobility-field coefficient $d\mu/dE$ is positive in the low-density gas, negative in the high-density gas and low-density liquid $[1.0 < (n/10^{21}) < 8]$, and positive in the normal liquid. The temperature coefficient of mobility $d\mu/dT$ is positive at all densities. The change of sign of $d\mu/dE$ going from $n = 0.9$ to 1.0 (10^{21} molecule/cm^3) is attributed to destructive interference of long-range attractive interactions, which tends to reduce the effective scattering cross sections at the lower velocities. The sign of $d\mu/dT$ remains positive because quasilocalization of electrons occurs at density fluctuations of suitable magnitude in this region of n. Quasilocalization is characterized by large negative values of $\Delta H'$ and $\Delta S'$, with $\Delta G' \simeq 0$. The density-normalized mobility μn changes by less than a factor of 2 while increasing n from the low-density gas to the liquid at $n = 7 \times 10^{21}$ molecule/cm^3. At $n > 8 \times 10^{21}$ the value of μn plunges, due to the formation of more stable localized states; field-assisted delocalization of the electrons causes $d\mu/dE$ to become positive again. Electron behavior in fluid ethane is quite different from that in fluid methane. The differences are attributed to the difference in molecular shape; methane is much more spherelike than ethane. The less spherelike molecule has a lower average scattering cross section for electrons at 300 K in the low-density gas, a Ramsauer-Townsend minimum in σ_v lying at a lower energy, a larger ratio of threshold drift velocity to the speed of sound v_d^{thr}/c_o, and more stable localized states of electrons in the liquid.

I. INTRODUCTION

Electron transport in fluid methane has recently been reported for wide ranges of fluid density and temperature.[1] To briefly characterize the transport behavior one may cite the deep Ramsauer-Townsend minimum in the scattering cross section at ~0.25 eV in the dilute gas, interference by the formation of quasilocalized electron states in the dense gas near the vapor-liquid coexistence curve, the stability of the quasifree state in the dense liquid, and a mobility maximum where the density-normalized mobility μn is 50 times the value in the low-density gas, at a density 1.8 times the critical, 1.8 n_c.

Methane is the simplest hydrocarbon molecule. It has tetrahedral structure and a nearly isotropic polarizability. The next-simplest hydrocarbon molecule might be considered to be ethane, $H_3C\text{-}CH_3$. The CH_3 groups can rotate relative to each other on the axle of the C-C bond. The molecule has a distinctly anisotropic polarizability. The wide-ranging study of electron transport in fluid methane[1] has been repeated in ethane. The purpose is to learn more about electron behavior in molecular fluids and to provide impetus for a theoretical treatment of the subject by those who are equipped to do so.

A small amount of work on electron scattering and transport in low-density ethane gas has been reported.[2-6] Agreement between results from different laboratories is not particularly good.

In liquid ethane, by contrast with methane, the quasifree state of electrons is not stable except near the critical region. A localized (solvated) state is formed.[6-8]

II. EXPERIMENTAL

A. Materials and techniques

Phillips Research Grade ethane (99.97%) was transferred to a grease-free vacuum line through flexible stainless-steel tubing that was welded to a Kovar-glass seal. About 50 ml of liquid-solid was degassed by trap-to-trap distillation under vacuum, while pumping on the liquid-nitrogen-cooled receiver. The ethane was then held overnight as a liquid at 195 K (Dry Ice: acetone) on Davison 3A Molecular Sieves. It was then degassed again and transferred onto a series of potassium mirrors, on which it was held at 195 K for two weeks. A fresh mirror was used every two days.

The mobility measurement systems were described earlier. Time-of-flight measurements were used,[9] except at the lowest temperatures, for which a conductance method was required.[10] The

distance between the parallel-plate electrodes was 3.2 mm.

B. Physical properties

Gas densities were taken from Ref. 11, and liquid densities from Ref. 12. Dielectric constants were calculated from the Lorenz-Lorentz equation,[13] using the refractive index from Ref. 14 as a base. The average polarizability and anisotropy of polarizability were calculated from data in Ref. 15. The speed of sound and isothermal compressibility were obtained from Ref. 16. Some of the properties of ethane are listed in Table I, along with those of methane[17] for comparison.

III. RESULTS

Electron mobilities were measured as functions of electric-field strength and temperature (or density) in the liquid and gas phases along the coexistence curve. The temperature and density are interdependent in the coexistence fluids. Measurements were also made in the gas as a function of temperature at several fixed densities.

A. Electric field

Earlier measurements[2,3,5,18] in ethane were of drift velocity v_d against density-normalized field strength E/n at room temperature, for a range of densities $n < 2.7 \times 10^{19}$ molecule/cm^3. These results are plotted as density-normalized mobilities μn along with the present data obtained at 294 K (Fig. 1). The value of μn increases slightly at $E/n > 0.06$ Td (Townsend), passes through a maximum at $E/n \approx 0.3$ Td, then decreases. The electron drift velocity v_d is nearly independent of field strength at 53 ± 3 km/s between 3 and 46 Td. Results from different laboratories agree to within 12% in the region of overlap. Differences are smaller at high fields (Fig. 1), where drift velocities are easier to measure precisely.

The threshold field strength $(E/n)_{thr}$, below which the electrons are in thermal equilibrium with the fluid, varies with temperature in the low-density gas (Fig. 2). Decreasing the temperature lowers the electron mean energy and the low-field mobility; electron heating by the field therefore becomes significant at progressively lower fields.

The effect of gas density upon the field effect is illustrated in Fig. 3. At high densities where multibody interactions are important, the magnitude of the positive $d\mu/dE$ decreases with increasing n and the threshold $(E/n)_{thr}$ increases. At $n > 1.0 \times 10^{21}$ molecule/cm^3 $d\mu/dE$ becomes negative and $(E/n)_{thr}$ decreases again. The variation of $(E/n)_{thr}$ with density in the saturated vapor (in equilibrium with the liquid) is shown in Fig. 4.

In the low-density liquid phase at $T \approx 290$ K and $n \approx 7 \times 10^{21}$ molecule/cm^3 it has previously been found that $(E/n)_{thr} \approx 0.1$ Td and $d\mu/dE$ is negative.[19] However, at $T \leq 216$ K and $n \geq 1.0 \times 10^{22}$ molecule/cm^3, $d\mu/dE$ is again positive and $(E/n)_{thr} > 0.5$ Td.[20] There are therefore two sign changes in the $(E/n)_{thr}$ vs n curve, one at 1.0×10^{21} and another near 9×10^{21} molecule/cm^3 (Fig. 4).

B. Density-normalized mobility

Figure 4 also shows μn vs n for thermal electrons in the coexistence fluids. At $n < 1.3 \times 10^{21}$ molecule/cm^3 μn is constant at 3.1×10^{23} molecule/cm V s within the experimental uncertainty of

TABLE I. Physical Properties.[a]

	CH_4	H_3CCH_3
$T_c(K)$	190.6	305.5
$n_c(10^{21}$ molecule/cm$^3)$	6.09	4.06
P_c(MPa)	4.60	4.88
ϵ_c	1.23	1.25
dipole moment (10^{-18} esu cm)	0.00	0.00
average polarizability (10^{-24} cm^3)	2.6	4.4
polarizability anisotropy (10^{-24} cm^3)	0.0	0.7
$r_{vdW}(10^{-8}$ cm)[b]	1.6	1.8
$\sigma_{av}(10^{-16}$ cm$^2)$, 300 K[c]	4.0	3.4

[a] References 11–17.

[b] Reference 14, using $r_{vdW} = 10^{-8}(0.099b)^{1/3}$ cm, where b is in units of cm^3/mol.

[c] Present work.

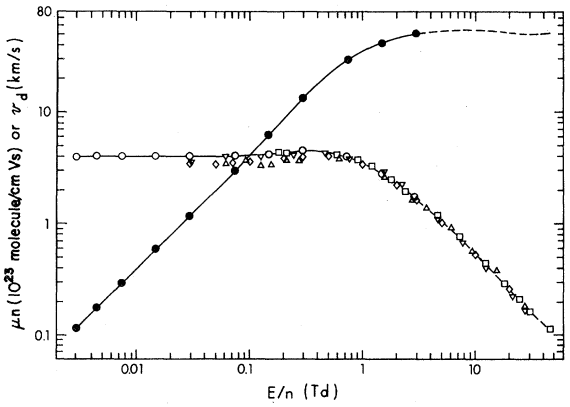

FIG. 1. Density-normalized mobility μn and drift velocity v_d as functions of the density-normalized electric-field strength E/n, in low-density ethane gas at $T \approx 295$ K. ●, v_d at $n = 6.8 \times 10^{19}$ molecule/cm^3 and $T = 294$ K, present work. μn: O, same as above; △, Ref. 2, 298 K, $0.4–7 \times 10^{18}$ molecule/cm^3; □, Ref. 3, 293 K, $0.6–8 \times 10^{17}$ molecule/cm^3; ▽, Ref. 5, 298 K, 3×10^{18} molecule/cm^3; ◇, Ref. 18, 295 K, 1.5×10^{19} molecule/cm^3.

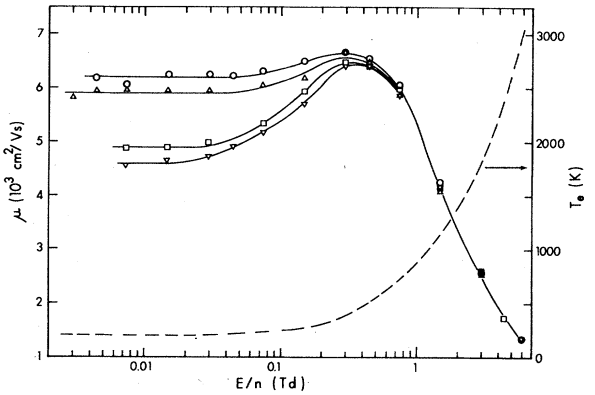

FIG. 2. Electron mobility plotted against E/n at $n = 6.8\times10^{19}$ molecule/cm^3. $T(K)$: ▽, 197; □, 221; △, 294; O, 326. ---- represents the electron temperature T_e, estimated for the 197 K sample at $E/n < 0.3$ Td and any sample at $E/n > 0.3$ Td.

~3%. At higher densities μn decreases, reaching a minimum of ~1.9×10^{23} molecule/cm V s at 3×10^{21} molecule/cm^3, then rises to a maximum of 3.1×10^{23} molecule/cm V s at 5.6×10^{21} molecule/cm^3, and decreases steeply at still higher densities.

Values of μn as a function of n in the gas at constant $T = 1.02T_c$ are nearly parallel to those in the coexistence vapors (Fig. 4). It should be remembered that the temperature difference between the constant T and coexistence curves decreases with increasing n, so the temperature coefficient of mobility increases with n in the gas phase.

C. Temperature

In the gas phase at constant density the thermal electron mobility has a positive temperature coefficient (Fig. 5). The coefficient increases with

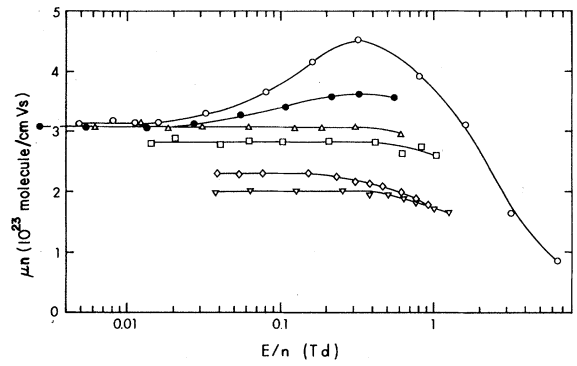

FIG. 3. Effect of gas density upon the field dependence of μn. The gases are in equilibrium with liquid at the temperature indicated. $T(K)$, $n(10^{19}$ molecule/cm^3): O, 193, 6.2; ●, 256, 57; △, 276, 102; □, 289, 150; ▽, 302, 246; ◇, 306, 406, critical fluid.

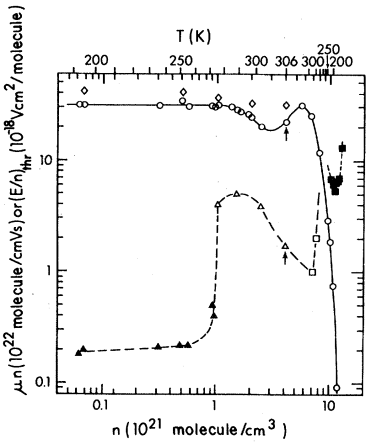

FIG. 4. $(E/n)_{thr}$, ▲△■□, and μn(thermal electrons), O, as functions of n in the coexistence vapor and liquid. The closed and open symbols indicate positive and negative values of $d\mu/dE$, respectively, at $E/n > (E/n)_{thr}$. □, Ref. 19; ■, Ref. 20. The arrow indicates n_c. ◇, μn at constant temperature $1.02T_c = 312$ K.

density, in confirmation of the result in Sec. III B. Although the Arrhenius model is inappropriate for transport in the low-density gas, the Arrhenius temperature coefficients are listed in Table II to give an overview of the magnitude of the effect of density.

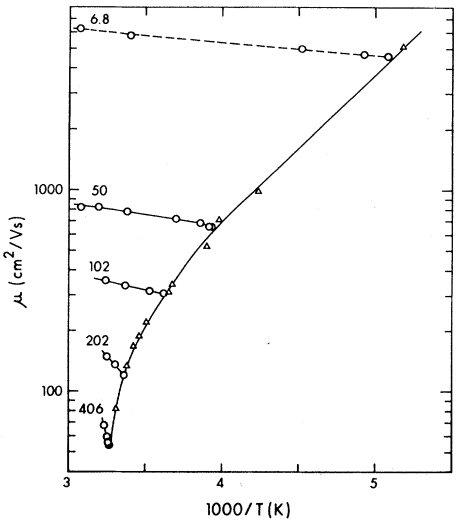

FIG. 5. Temperature dependence (Arrhenius plot) of thermal-electron mobilities in the gas phase along the coexistence curve (△) and at several constant densities (O). The numbers labeling the curves are $n/10^{19}$ molecule/cm^3. The dashed line was calculated using Eq. (2) and the cross sections represented by the full line or long-dash line in Fig. 7.

TABLE II. Temperature coefficients of thermal-electron mobilities in ethane at different densities.

n (10^{19} molecule/cm^3)	$\frac{n}{n_c}$	T range (K)	E_μ (kJ/mol)	μ_n^0[a] (cm^2/V s)	$-\Delta H'$[b] kJ/mol	$-\Delta S'$[b] (J/mol K)	$\Delta G'$[c] (kJ/mol)	$S(0)$[d]	$\Delta S'/S(0)$ (J/mol K)
6.8	0.017	197–326	1.3					1.0	
50	0.123	254–325	2.4					1.4	
102	0.25	276–309	3.8	490	9	36	+2	2.5	14
202	0.50	298–308	16	250	33	109	0	5.7	19
406	1.00	307–310	60	160	106	340	−2	33	10

[a] Rough estimates, see text.
[b] Equation (9).
[c] $\Delta G' = \Delta H' - T\Delta S'$
[d] $S(0) = nkT\chi_T = 0.083T/(\mathrm{DP/DD})$, see Ref. 16.

As the temperature is increased along the gas-liquid coexistence curve the gas density increases rapidly. The density effect dominates and μ decreases (Fig. 5).

In the liquid phase the mobility increases with temperature (Fig. 6). As the critical region is approached the mobility increases sharply, then passes through a slight maximum at $(T_c - 2) = 304$ K. At $T > T_c$, with $n = n_c$, the mobility increases again.

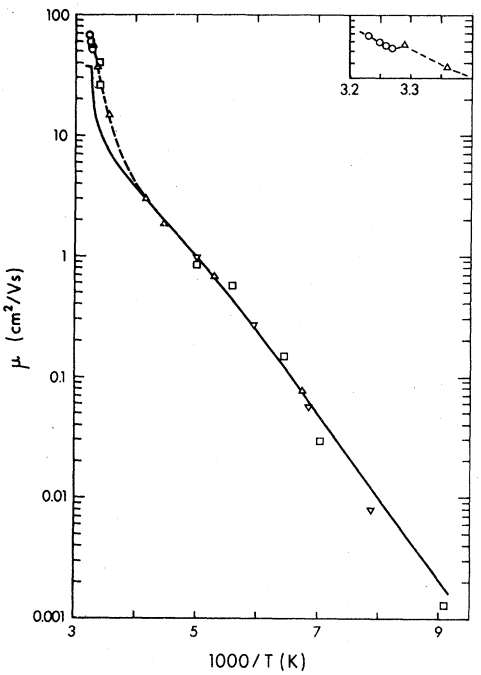

FIG. 6. Arrhenius plot of thermal-electron mobilities in liquid ethane. △, present work; □, Ref. 20; ▽, Ref. 7; ○, supercritical gas at $n = n_c$, present work. The solid line was calculated from Eqs. (10)–(15), using $\mu_{il}^0 = 0.04$ cm^2/V s, $E_{il} = 0.04$ eV, $E_0(\mathrm{eV}) = 0.60 - 0.0012T$, $\sigma = 0.050 + 0.0010T$, and $\mu_h^0 = 74(0.549/b_T)^2(185/T)$.

IV. DISCUSSION

A. Low-density gas

1. Temperature dependence at low fields

The variation of the mobility with temperature in the low-density gas reflects the energy dependence of the scattering cross section. The electron scattering cross section of ethane possesses a Ramsauer-Townsend minimum in the vicinity of 0.1 eV.[4,5] However, the reported[4,5] energy dependences of the cross section differ greatly in magnitude.

The mobility μ_{id} of electrons in the low-density gas can be expressed as[21]

$$\mu_{id} = -\frac{4\pi e}{3mn}\int_0^\infty \frac{v^2}{\sigma_v}\frac{df_0}{dv}\,dv\,, \tag{1}$$

where e and m are the charge and mass of the electron, respectively, n is the number of molecules/cm^3, σ_v is the scattering cross section of the molecule for electrons of velocity v, and f_0 is the spherically symmetric term in the series expansion of the electron velocity distribution function. At low fields the distribution is Maxwellian. One then has

$$\mu_{id} = (5.23\times10^{-14}/nT^{2.5}) \times \int_0^\infty (v^3/\sigma_v)\exp[(-3.30\times10^{-12})v^2/T]dv \tag{2}$$

The values of σ_v as a function of v were determined by fitting Eq. (2) to the sets of (μ, T) values for $n = 6.8\times10^{19}$ molecule/cm^3 (Fig. 5). The equation was integrated numerically, using 31 logarithmic steps between $v = 3\times10^6$ and 3×10^7 cm/s. The fitting procedure is described in Ref. 22.

The energy range of greatest sensitivity in the cross-section–mobility fitting procedure is that near the maximum in the integrand in Eq. (2). The integrand is represented by F in Fig. 7 and is displayed for 260 K, using the full curve for σ_v. The temperature 260 K is near the center of the range

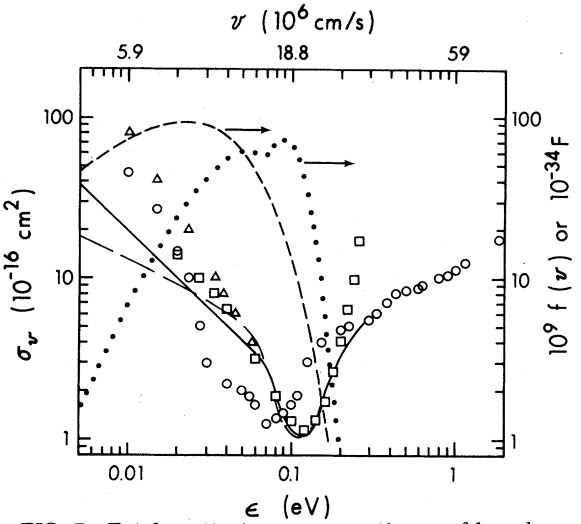

FIG. 7. Total scattering cross section σ_v of low-density ethane gas as a function of electron energy ϵ and velocity v. The solid line and long-dash line represent cross sections that produce the dashed line in Fig. 5. Previous values of cross sections are from Refs. 2 (△), 4 (○), and 5 (□). --- represents $f(v)=N^{-1}dN(v)/dv$ for a Maxwellian distribution of electrons at 260 K, where $f(v)dv$ is the fraction of electrons that have velocities between v and $v+dv$. ···, $F=(v^3/\sigma_v)\exp(-3.3\times10^{-12}v^2/T)$, at 260 K. F is inversely proportional to the probability of a scattering event, weighted for the velocity distribution at a given T.

197–326 K used for the low-density gas. The most sensitive energy region is about 0.015–0.15 eV. The accuracy of the cross sections estimated from the present mobilities decreases with increasing distance from this central region. However, the values of Duncan and Walker[4] at 0.5–2 eV, obtained from D/μ measurements, provide a reasonable upper end to the curve. Their technique was less accurate at the lower energies.

The solid curve and the long-dash curve in Fig. 7 are reasonable limits for the present results.

The averaging procedure appropriate to cross sections derived from mobilities is[23]

$$\sigma_{av}=\langle v\rangle/\langle v/\sigma_v\rangle\,, \tag{3}$$

which for a Maxwellian distribution of velocities becomes

$$\sigma_{av}=\frac{(4.59\times10^{22})T^2}{\int_0^\infty(v^3/\sigma_v)\exp[(-3.3\times10^{-12})v^2/T]dv}\,. \tag{4}$$

For ethane at 200 and 300 K, $\sigma_{av}=5.4$ and 3.4 (10^{-16} cm^2), respectively. These are smaller than the corresponding values for methane, 5.9 and 4.0 (10^{-16} cm^2).[1] The larger cross sections for methane are related to the greater degree of sphericity of that molecule, which seems to cause the Ramsauer-Townsend minimum in the scattering cross section to lie at a higher energy (~0.25 eV).[1]

The average scattering cross sections of methane and ethane do not reflect the relative values of the mean polarizabilities or of the van der Waals (vdW) radii (Table I). The molecular shape dominates the relative electron scattering powers of these molecules, but the reason for this is not known.

2. *Field effect*

At temperatures near 200 K the mobility is independent of applied electric-field strength at $E/n<0.02$ Td (Fig. 2). Under these circumstances the electrons remain near thermal equilibrium with the gas. At higher field strengths there is a net gain of energy by the electrons, and they heat up. By using the crude approximation that the electron energy distribution remains Maxwellian, Eq. (2) and the cross-section curve in Fig. 7 (using Duncan and Walker's values[4] at $\epsilon>0.3$ eV) can be applied to the measured electron mobilities in Fig. 2 to calculate the electron temperature T_e as a function of E/n. The results obtained are displayed in Fig. 2, using the 197 K sample at low fields and any sample at $E/n>0.3$ Td. The values of T_e at 1 and 6 Td are 870 and 3000 K, respectively, compared to the values 780 and 2800 K estimated from the D/μ values of Duncan and Walker.[4]

The calculations revealed that the thermal electron mobility would be independent (within ±1%) of temperature between 390 and 550 K.

The product of the threshold field and the thermal electron mobility gives the threshold drift velocity $v_d^{\rm thr}$. The magnitude of $v_d^{\rm thr}$ is related to, among other things, the ability of the fluid molecules to remove collisionally from the electrons the energy that they acquire by acceleration in the field between collisions. The parameter $v_d^{\rm thr}/c_0$, where c_0 is the speed of low-frequency sound in the fluid, is useful in assessing the relative contributions of elastic and inelastic scattering processes to electron-molecule energy exchange at thermal and near thermal energies.[1] When elastic scattering is the dominant process that moderates the electron energy, $v_d^{\rm thr}/c_0\approx1$.[24] The value of the ratio increases as the contribution of inelastic scattering increases.[1,25] These parameters are larger when the molecules are less spherelike and more flexible.[1]

In ethane at 197 K and 6.8×10^{19} molecule/cm^3, $v_d^{\rm thr}=620$ m/s and $c_0=251$ m/s,[16] so $v_d^{\rm thr}/c_0=2.5$. The ratio increases with temperature at this density, and at 326 K equals 2500/321 = 7.9 (Fig. 2 and Ref. 16). The larger electron energies, and possibly the greater amounts of rotational and vibrational excitation in the molecules, at the higher temperatures enhance the probability of inelastic energy exchange.

B. Effect of density

The density of the coexistence vapor (in equilibrium with liquid) increases with increasing temperature. The increase of μn with temperature that might be expected on the basis of single-body interactions is scarcely noticeable in the coexistence vapor (Fig. 4) because multibody effects become dominant at relatively low temperatures.

The dip in the μn curve at $n > 1.3 \times 10^{21}$ molecule/cm^3 in the vapor has been attributed to quasilocalization of electrons within density fluctuations[1,26]:

$$\text{medium} \rightleftharpoons \text{site}, \tag{5}$$

$$e_{qf}^- + \text{site} \rightleftharpoons e_{ql}^-, \tag{6}$$

where "site" represents a density fluctuation of sufficient amplitude and appropriate breadth, while e_{qf}^- and e_{ql}^- represent the quasifree and quasilocalized electron, respectively. The term quasilocalized is preferred to localized for e_{ql}^-, because the state appears to be highly transient and the net effect on the average mobility of the electrons is much smaller than that of the localization process that occurs in the liquid at $n > 7 \times 10^{21}$ molecule/cm^3 (Fig. 4).

1. Temperature effects in dense gases at constant density

In the gas the magnitudes of the density fluctuations, and hence the concentration of quasilocalization sites, is greatest in the coexistence vapor.

The density normalized mobility at any value of n and T is

$$\mu n = n \mu_n^0 f, \tag{7}$$

where μ_n^0 is the quasifree electron mobility at density n and

$$f = [e_{qf}^-]/([e_{qf}^-] + [e_{ql}^-]) = (1 + [\text{site}] K_6)^{-1}, \tag{8}$$

where [site] is the concentration of sites and K_6 is the equilibrium constant of reaction (6). It follows that

$$(n \mu_n^0/\mu n) - 1 = \exp(\Delta S'/\mathcal{R}) \exp(-\Delta H'/\mathcal{R}T), \tag{9}$$

where $(\Delta H' - T\Delta S') = \Delta G'$ is the standard Gibbs free energy of the overall $e_{qf}^- + \text{medium} \rightarrow e_{ql}^-$ quasilocalization process, $\Delta S' = \Delta S_5^0 + \Delta S_6^0 \approx \Delta S_5^0$ and $\Delta H' = \Delta H_5^0 + \Delta H_6^0 \approx \Delta H_5^0$.[1]

Plots of $\ln[(n\mu_n^0)/\mu n) - 1]$ against T^{-1} give $\Delta H'$ from the slope and $\Delta S'$ from the intercept. The problem is to estimate reasonable values of μ_n^0. For methane,[1] the measurements of Lehning[27] at high pressures, room temperature (~293 K, which is $\gg T_c = 191$ K), and $E/n = 0.06$ Td made possible reasonable estimates of μ_n^0 in that gas. However, the analogous measurements of Huber[18] in ethane at 295 K, which is $< T_c = 306$ K, cannot be used to obtain μ_n^0 in the high-density gases. By comparison with the behavior in methane[1] and neopentane,[23,28] rough values of $n\mu_n^0$ were taken to be 5×10^{23} molecule/cm V s at $n = 1 \times$ and 2×10^{21} molecule/cm^3, and 6.5×10^{23} at $n_c = 4.1 \times 10^{21}$. The increase of μn at $n > 3 \times 10^{21}$ (Fig. 4) is due to conduction band formation, which increases $n\mu_n^0$. The obtained values of $\Delta H'$ and $\Delta S'$ are listed in Table II. As in methane,[1] $\Delta H'$ is approximately double the experimentally measured Arrhenius temperature coefficient E_μ (Table II). The values of $\Delta H'$ and $\Delta S'$ are large and negative, in agreement with the proposed quasicondensation that is involved in the formation of a site [reaction (5)]. The values of $\Delta S'$ correlate roughly with the structure factor $S(0) = nkT\chi_T$ in the dense gases away from the critical region; the ratio $\Delta S'/S(0)$ has values in the vicinity of -15 J/mol K, similar to those in methane.[1]

The values of $\Delta G'$ are near zero (Table II), in agreement with the relatively small extent of the quasilocalization process.

2. Results of forcing the behavior in dense gases into the single-scatterer model

The electron mobilities at the different temperatures were fitted to Eq. (2) for each of the gas densities displayed in Fig. 5. The purpose was to determine how the apparent scattering cross sections would be altered from those at low density. As an anchor point for the apparent σ_v distributions, the value at 0.08 eV was kept constant to as high a density as possible. The results displayed in Fig. 8 correspond to the curves drawn in Fig. 5.

Increasing the density to $n/n_c = 0.25$ had the effect of greatly raising the apparent cross sections at low energies, while slightly lowering the cross section at the minimum. The empirical effect was to triple the Arrhenius coefficient E_μ (Table II) while the value of μn in the coexistence vapor remained unchanged (Fig. 4). Further increase of the density to $n = 0.50 n_c = 202 \times 10^{19}$ molecules/cm^3 caused a violent shift in the apparent cross sections, in the same direction as the gentler shifts at lower densities (Fig. 8). The violent shift signals a change of mechanism, which becomes more extensive at $n = n_c$ (Fig. 8). The sharp cutoff in scattering cross section at a high energy leads to a scattering model that is mathematically equivalent to the Arrhenius activation model of transport. This is because the Maxwellian distribution is exponential at $\epsilon \gg kT$ and the apparent scattering cross section is nearly a delta function.

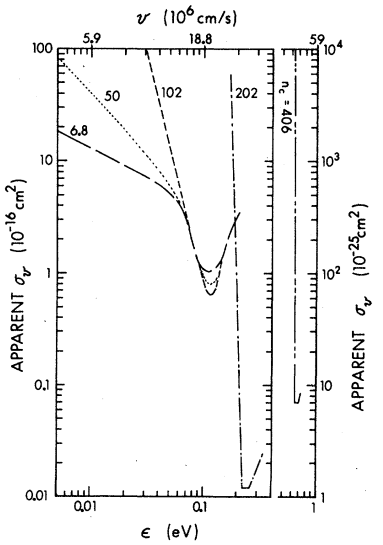

FIG. 8. Effect of gas density upon the apparent scattering cross sections, which were obtained by fitting the single-scatter equation (2) to the mobilities at each density (Fig. 5). The numbers labeling the curves are $n/10^{19}$ molecule/cm^3.

At $n=50$ and 102 (10^{19} molecule/cm^3), the gradual increase of the apparent scattering cross sections at low energies (Fig. 8) signals the faint beginnings of the quasilocalization process. If the change in apparent cross section had been due to the mutual interference of long-range attractive scattering interactions of individual molecules, the cross sections at low energies would have been expected to decrease rather than increase.[31]

Figure 8 is a dramatic representation of the change of transport mechanism that occurs with increasing gas density.

3. Liquid phase

As the density of the coexistence fluid is increased through the critical to the liquid phase, μn increases to a maximum of 3.1×10^{23} molecule/cm V s at $n=1.4n_c=5.5\times10^{21}$ molecule/cm^3 (Fig. 4). Further increases of density cause μn to decrease, due to the formation of localized electron states. No special behavior was noted in the critical region, indicated by the arrow in Fig. 4.

In the liquid at temperatures well below the critical the electron mobility can be fit by a two-state model.[29,30] The relevant equations have been discussed earlier[30] and are simply listed here:

$$\mu=(1-\chi)\mu_{il}^0\exp(-E_{il}/kT)+\chi\mu_h^0, \tag{10}$$

where χ is the fraction of electrons that are in the high mobility state with mobility μ_h^0, while μ_{il}^0 and E_{il} are, respectively, the preexponential factor and activation energy of mobility in the localized (ionlike) state:

$$\chi=\int_{-\infty}^{\infty}N(E)[1+\exp(E/kT)]^{-1}dE\,, \tag{11}$$

$$N(E)=\pi^{-1/2}\sigma^{-1}\exp[-(E-E_0)^2/\sigma^2] \tag{12}$$

$$E_0=E(0)-aT\,, \tag{13}$$

$$\sigma=\sigma(0)+bT\,, \tag{14}$$

$$\mu_h^0=\mu_{\rm ref}^0(b_{\rm ref}/b_T)^2(T_{\rm ref}/T)\,, \tag{15}$$

where $b_{\rm ref}$ is the liquid density at $T_{\rm ref}$. Equations (13)–(15) are adequate when the electron localization energy is $\gg kT$, but they usually break down as the critical region is approached.[30] Attention is therefore focused on the normal liquid.

The parameters in Eqs. (13)–(15) cannot be uniquely determined without an extra, not yet available, source of information. To reduce the plasticity of the calculations and to facilitate comparison between systems, most of the variability is arbitrarily forced into a, $\sigma(0)$, and b. The value $E(0)=0.60$ eV used for several other hydrocarbons[32,33] is retained for ethane. By taking μ(localized electron) $\gtrsim 2\mu$(molecular cation)[29] and using data from Ref. 34, we obtained $\mu_{il}^0\approx0.04$ cm^2/V s and $E_{il}\approx0.04$ eV for liquid ethane. A negligible amount of transport occurs in the localized state except at $T<130$ K. We chose $T_{\rm ref}=185$ K, the normal boiling point of ethane, and $\mu_{\rm ref}^0=74$ cm^2/V s, which is roughly a minimum value at allows a reasonable fit to the experimental mobility curve when $E(0)=0.60$ eV is used. The closest fit obtained is shown in Fig. 6, with E_0(eV) $=0.60-0.0012T$ and σ(eV) $=0.050+0.0010T$.

4. Field effect

The two changes of sign of $d\mu/dE$ indicated in the $(E/n)_{\rm thr}$ vs n plot (Fig. 4) have different causes. The discontinuity in the dense gas at $n=1.0\times10^{21}$ molecule/cm^3 is associated with the density dependence of the electron scattering cross section σ_v as a function of velocity v. When the weighted values of σ_v sampled over the Maxwellian distribution of velocities vary more rapidly than v^{-1}, that is, when $\alpha>1.0$ in $\sigma_v\approx A_\alpha v^{-\alpha}$, then $d\mu/dT$ and $d\mu/dE$ [just above $(E/n)_{\rm thr}$] are positive. The temperature and field coefficients become zero when $\alpha=1.0$, and negative when $\alpha<1.0$. The sign change at 1.0×10^{21} molecule/cm^3 is consistent with the low-energy wing of the σ_v curve (Fig. 7) being due to a long-range attractive interaction with a single molecule. At densities near 1×10^{21} the molecules are sufficiently close together that the attractive interactions tend to destructively interfere with

each other, thereby lowering the effective cross section σ_{eff} and decreasing the effective velocity exponent α_{eff}. As α_{eff} passes through 1.0 the electrons must be raised to significantly higher energies for a field effect to be noticeable, so $(E/n)_{thr}$ increases (Fig. 4). At higher densities the value of α_{eff} becomes progressively smaller than 1.0, the magnitude of the field effect increases, and the threshold may be observed at lower fields (Fig. 4).

At $n > 8 \times 10^{21}$, electron localization dominates the transport process and the field effect changes sign again. The positive sign of the field coefficient is attributed to field-assisted delocalization of the electron.

Only the first of these two sign changes, positive to negative with increasing density, is observed in methane.[1] Electron localization does not occur in methane, (distinct from quasilocalization, which can occur in all fluids studied to date). The change of sign of $d\mu/dE$ from positive to negative with increasing density occurs at $n > n_c$ in methane[1] and at $n < n_c$ in ethane. This is due to the fact that the less spherelike molecule ethane has a minimum cross section σ_{min} at a lower energy.

We do not attribute the sign change of $d\mu/dE$ to a shifting of σ_{min} towards lower energies, but to the lowering of the low-energy wing with increasing density. The location of σ_{min} may be assumed to be little affected by gas densities in the region of 1.0×10^{21} molecule/cm^3.

Perhaps it should be emphasized that the real changes in the low-energy wing of σ_v with increasing density are in the opposite direction to those indicated by the "apparent σ_v" in Fig. 8. The quasilocalization process causes $d\mu/dT$ to be positive, mainly through the temperature effect on equilibrium (8). The electric field does not affect this equilibrium, so the temperature and field can have coefficients with opposite signs when quasilocalization is a near-dominating process.

ACKNOWLEDGMENTS

We would like to thank the staff of the Radiation Research Center for aid with the electronics. This research received financial assistance from the Natural Science and Engineering Research Council of Canada.

[1] N. Gee and G. R. Freeman, Phys. Rev. A 20, 1152 (1979).
[2] C. R. Bowman and D. E. Gordon, J. Chem. Phys. 46, 1878 (1967).
[3] T. L. Cottrell, W. J. Pollock, and I. C. Walker, Trans. Faraday Soc. 64, 2260 (1968).
[4] C. W. Duncan and I. C. Walker, J. Chem. Soc. Faraday Trans. 2 70, 577 (1974).
[5] D. L. McCorkle, L. G. Christophorou, D. V. Maxey, and J. G. Carter, J. Phys. B 11, 3067 (1978).
[6] N. Gee and G. R. Freeman, Chem. Phys. Lett. 60, 439 (1979).
[7] M. G. Robinson and G. R. Freeman, Can. J. Chem. 52, 440 (1974).
[8] W. F. Schmidt, G. Bakale, and U. Sowada, J. Chem. Phys. 61, 5275 (1974).
[9] J.-P. Dodelet and G. R. Freeman, Can. J. Chem. 55, 2264 (1977).
[10] J.-P. Dodelet and G. R. Freeman, Can. J. Chem. 50, 2667 (1972).
[11] L. N. Canjar and F. S. Manning, *Thermodynamic Properties and Reduced Correlations for Gases* (Gulf, Houston, 1967).
[12] R. W. Gallant, *Physical Properties of Hydrocarbons* (Gulf, Houston, 1968), Vol. 1.
[13] N. E. Hill, W. E. Vaughan, A. H. Price, and M. Davies, *Dielectric Properties and Molecular Behavior* (Van Nostrand Reinhold, Toronto, 1969), p. 191.
[14] *Handbook of Chemistry and Physics*, 50th ed., edited by R. C. Weast (Chemical Rubber, Cleveland, 1969).
[15] R. J. W. Le Fevre, Rev. Pure Appl. Chem. 20, 67 (1970).
[16] R. D. Goodwin, H. M. Roder, and G. C. Straty, *Thermodynamic Properties of Ethane, from 90 to 600 K at Pressures to 700 Bar*, NBS Technical Report No. 684 (U.S. GPO, Washington D.C., 1976).
[17] S. Angus, B. Armstrong, and K. M. De Reuck, *International Thermodynamic Tables of the Fluid State-5: Methane*, IUPAC Chemical Data Series No. 16 (Pergamon, Oxford, 1978).
[18] B. Huber, Z. Naturforsch. 24a, 578 (1969).
[19] W. Döldissen, G. Bakale, and W. F. Schmidt, (a) Chem. Phys. Lett. 56, 347 (1978); (b) J. Electrostatics 7, 247 (1979).
[20] W. F. Schmidt, G. Bakale, and U. Sowada, J. Chem. Phys. 61, 5275 (1974).
[21] L. G. H. Huxley and R. W. Crompton, *The Diffusion and Drift of Electrons in Gases* (Wiley, New York, 1974), Chap. 3.
[22] G. R. Freeman, I. György, and S. S.-S. Huang, Can. J. Chem. 57, 2626 (1979) and references therein. In Ref. 1 the equivalent symbols are $(1-j)=\alpha$ and $b_j = A_\alpha^{-1}$.
[23] I. György and G. R. Freeman, J. Chem. Phys. 70, 4769 (1979).
[24] W. Shockley, Bell Syst. Tech. J. 30, 990 (1951), pp. 1018–1024.
[25] B. V. Paranjape, Phys. Rev. A 21, 405 (1980).
[26] S. S.-S. Huang and G. R. Freeman, J. Chem. Phys. 68, 1355 (1978).
[27] H. Lehning, Phys. Lett. 29A, 719 (1969).
[28] S. S.-S. Huang and G. R. Freeman, J. Chem. Phys. 69, 1585 (1978).

[29]J.-P. Dodelet and G. R. Freeman, Can. J. Chem. 53, 1263 (1975).
[30]J.-P. Dodelet and G. R. Freeman, Can. J. Chem. 55, 2893 (1977).
[31]V. M. Atrazhev and I. T. Iakubov, J. Phys. D 10, 2155 (1977).
[32]S. S.-S. Huang and G. R. Freeman, Can. J. Chem. 56, 2388 (1978).
[33]T. G. Ryan and G. R. Freeman, J. Chem. Phys. 68, 5144 (1978).
[34]N. Gee and G. R. Freeman, Can. J. Chem. (in press) "Cation Mobilities in Liquid and Supercritical $C_1 - C_4$ Hydrocarbons".